GEOPHYSICAL RESEARCH LETTERS, VOL. 28, NO. 16, PAGES 3171-3174, AUGUST 15, 2001

Seasonal dependence of surface wind stress variability on SST and precipitation over the tropical Pacific

Fanglin Yang, Arun Kumar, and Wanqiu Wang

Environmental Modeling Center, National Centers for Environmental Prediction, Washington D.C.

Abstract. The dependence of interannual variability of surface zonal and meridional wind stresses (τ_x and τ_y) on sea-surface temperature (SST) and precipitation over the tropical Pacific is examined using observed data. A strong seasonality in the dependence is found. In January, the largest SST and precipitation anomalies are located in the central to eastern and central tropical Pacific respectively. τ_x anomalies in the southern central tropical Pacific and τ_y anomalies in the northern tropical Pacific are highly correlated to both the SST and precipitation anomalies. In contrast, during July the largest SST and precipitation anomalies are located at the eastern and western tropical Pacific respectively. East of the dateline, τ_x anomalies present little dependence on the SST anomalies. West of the dateline, τ_x anomalies depend strongly on the precipitation anomalies that are not linked to the leading modes of SST.

1. Introduction

The impact of El Niño - Southern Oscillation (ENSO) on the global atmosphere has been extensively investigated and is relatively well understood, however, the prediction of ENSO events itself still presents a challenge [*Trenberth et al.*, 1998; *Stockdale et al.*, 1998]. A hierarchy of coupled ocean and atmosphere models with various complexity have been developed to understand and to predict ENSO events. Within this hierarchy the simplest are the *intermediate* coupled models, in which a simplified ocean is coupled to a simple representation of wind stress in terms of anomalous sea-surface temperature (SST) [e.g., *Zebiak and Cane*, 1987]. The next category of coupled models, referred to as *hybrid* models, employs an oceanic GCM coupled to a statistical atmosphere [e.g., *Barnett et al.*]. The most complicated models are the coupled oceanic and atmospheric general circulation models (GCM) [e.g., *Ji et al.*, 1994; *Kirtman et al.*, 1996].

One of the key issues to successfully simulate and predict ENSO events is how well the surface wind stress climatology, as well as its interannual variability over the tropical Pacific, is modeled. A related question is what factors determine the surface wind stress variability over the tropical Pacific on monthly and longer time scales. The formation of the time mean surface wind stress over the tropics has been studied in relative detail [e.g., *Gill*, 1980; *Lindzen and Nigam*, 1987], although it is still in debate as to what extent the surface wind stress climatology is determined either by the SST gradients or by the convective heating. Less attention has been paid to the dependence of surface wind stress anomalies on SST and convective heating (or precipitation), and its seasonality. In this study we explore this question in further detail.

Paper number 2001GL013154.
0094-8276/01/2001GL013154$05.00

2. Data and Analyses

We use three independent data sets in our analysis, namely, the Florida State University (FSU) surface wind stress [*Goldenberg and O'Brien*, 1981], a blended dataset of SST [*Reynolds and Smith*, 1994; *Smith et al.*, 1996], and *Xie and Arkin* [1997] precipitation. The FSU dataset includes both zonal and meridional wind stresses from a subjective analysis of monthly ship observations over the tropical Pacific, and spans from 1961 to 1999. The blended SST dataset combines two sources. The first is reconstructed by fitting in situ data for the 1950-1980 period based on empirical-orthogonal function (EOF) analysis [*Smith et al.*, 1996]. The second is a global SST analysis constructed by combining in situ and satellite observations using optimum interpolation [*Reynolds and Smith*, 1994], and covers the period from 1981 to 1999. The observed precipitation covers the period from 1979 to 1999.

We performed the analyses using monthly mean SST, precipitation, surface zonal wind stress (τ_x) and surface meridional wind stress (τ_y) in the tropical Pacific (120°E – 80°W; 15°S – 10°N) from January 1979 through December 1999. Monthly mean anomalies are calculated relative to their respective 1979-1999 means. To emphasize seasonal characteristics of the preferred modes of variability and the relative roles of SST and precipitation in determining the variability of surface wind stresses, we performed analyses for each month and for each field respectively. Attention is paid to the comparison between the analyses for January and July. We performed the analysis using both EOFs and singular value decomposition, and found that the two approaches give similar conclusions. Here the analysis based on EOFs alone is presented.

To take the advantage of its longer record, we also use the NCEP/NCAR Reanalysis from 1958 through 1999 [*Kalnay et al.*, 1996] to examine the relationships among the interannual variabilities of surface wind stress, precipitation and SST.

3. Results

Fig. 1 shows the leading EOFs of SST, precipitation, τ_x and τ_y for January and July, respectively. For each field the leading mode for January explains larger variance than for July. The largest SST anomalies are centered at the equator at 130°W in January and at 5°S near the western coast of South America in July. In contrast, precipitation anomalies move northward from January to July along with the movement of

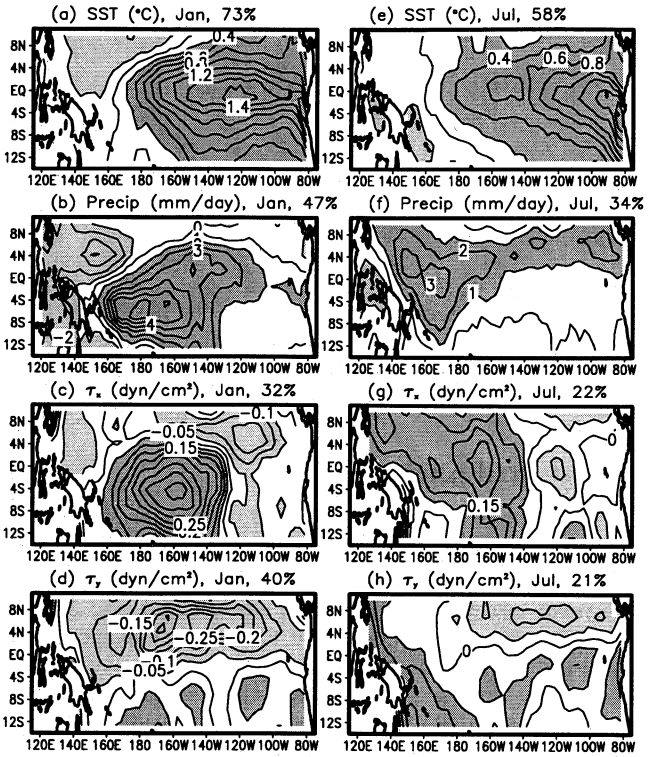

Figure 1. Leading EOFs of SST, precipitation, τ_x and τ_y in January and July. On each panel, the percent variance explained by the leading EOF to the total variance of the field is given. The contours show the typical magnitude of the anomalies.

the inter-tropical convergence zone. In January, the pattern of τ_x anomalies coincides well with the pattern of precipitation anomalies, with the former centered at about the dateline and 5°S and the latter at about 160°W and 5°S. The largest τ_y anomalies are found in the central to the eastern tropical Pacific at about 5°N. In July, the largest τ_x anomalies are located at 170°W at the equator, and 30° east of the center of precipitation anomalies. In the eastern tropical Pacific, there are no large τ_x anomalies though large precipitation anomalies do exist. Weak τ_y anomalies exist in the eastern tropical Pacific at about 8°N.

To what degree are the leading modes of τ_x and τ_y variability linked to those of SST and precipitation variability? Plotted in Fig. 2 are the time series of the normalized leading principle components (PCs) for τ_x, SST and precipitation (2a and 2b) and for τ_y, SST and precipitation (2c and 2d). Both τ_x and τ_y are better synchronized with precipitation and SSTs in January than in July. To quantify, in Table 1 the correlation coefficients between the leading-mode PCs of surface wind stresses, SST and precipitation are shown. In January, all the correlations are higher than 0.8. In July, the leading mode of τ_x no longer evolves in phase with the leading mode of SST, and the correlation between their PCs is only 0.39. The correlation between the PCs of τ_x and precipitation is 0.63, which is also much smaller than that in January. The PC of τ_y also evolves less coherently with the PCs of SST and precipitation in July than in January, however, compared to τ_x, the seasonality in the dependence of τ_y on SST and precipitation is not so evident. Throughout the year τ_y and precipitation anomalies have strong in phase relationship.

In general, the correlation coefficients between the leading-mode PC of τ_x and the leading-mode PC of SST or precipitation are smaller in boreal spring and summer than in boreal autumn and winter. The lowest correlation coefficients are found in boreal spring. This is probably a reason why some ENSO forecast models have lower forecast scores in boreal spring.

To explore linkages of wind stresses with precipitation and SSTs further, we correlated precipitation at each grid point with the leading-mode PC of SST, and τ_x and τ_y at each grid point with the leading-mode PCs of precipitation and SST. While the former analysis is to explore the association of precipitation with SST, the latter is used to investigate the associations of surface wind stresses with SST and precipitation. In Fig. 3 these analyses are shown as correlation maps.

In both January and July, precipitation correlates well with the leading mode of SST variability in the central to eastern tropical Pacific. Over the warm pool region, however, the precipitation variability during July (Fig. 1f) is not well correlated with the leading mode of SST variability. Further analysis shows that precipitation variability over the warm pool region as in Fig. 1f is not well correlated with the next 2 modes of SST variability either.

It is evident that SST and precipitation play a much more important role in determining the variability of surface wind stresses in January than in July. In January, τ_x anomalies in the central tropical Pacific and τ_y anomalies in the northern tropics correlate significantly with the leading modes of precipitation and SST. The patterns of correlation for τ_x and τ_y also coincide with the leading EOFs of τ_x and τ_y (Figs. 1c and 1d). During July, in contrast, correlation patterns for τ_x and τ_y anomalies with the leading modes of SST and precipitation do not present a consistent and coherent picture.

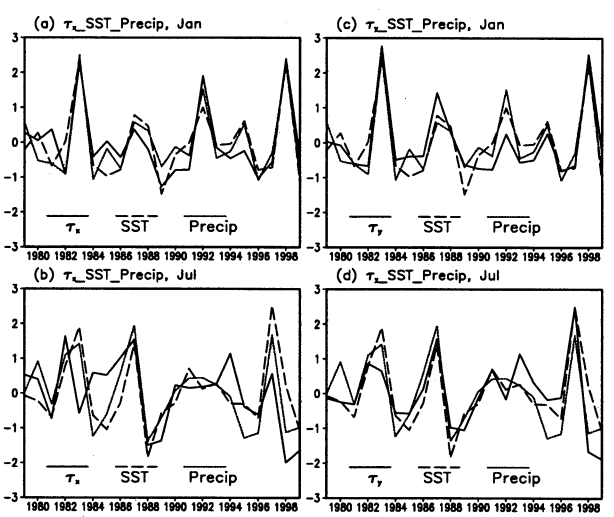

Figure 2. Time series of the PCs of the leading EOFs of τ_x (a and b) and τ_y (c and d) along with the PCs of the leading EOFs of SST and precipitation in January and July. Each PC is normalized by its own standard deviation.

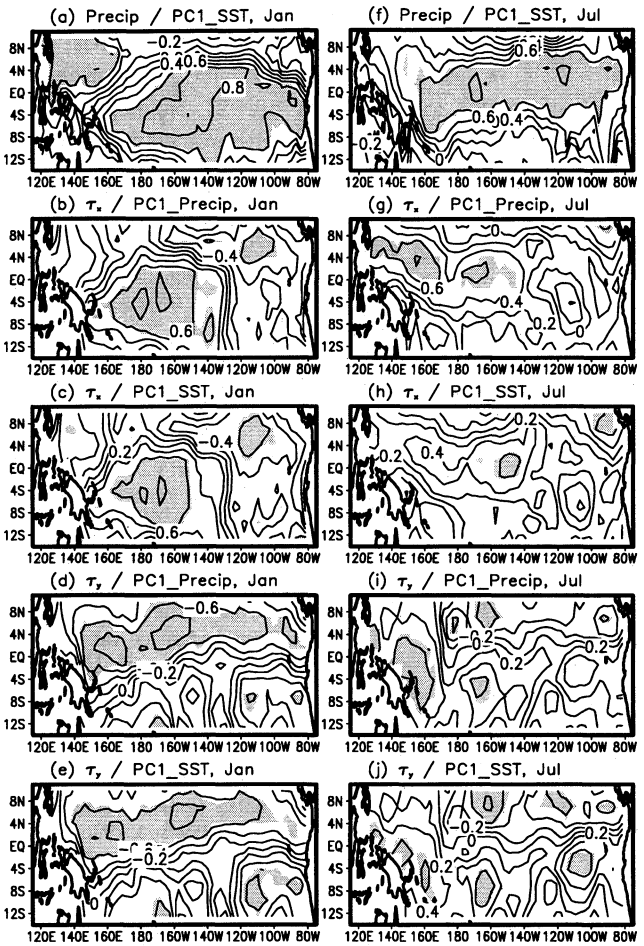

Figure 3. Correlation coefficients between a given field at each grid point and the leading mode PC of the other. (a) and (f): precipitation and the PC of SST; (b) and (g): τ_x and the PC of precipitation; (c) and (h): τ_x and the PC of SST; (d) and (i): τ_y and the PC of precipitation; (e) and (j): τ_y and the PC of SST. Areas with correlations significant at the 1% level for a Student's t-test are shaded. The contour interval is 0.2.

For τ_x, while only a small region centered at about 170°W has significant correlation with the PC of SST, significant correlation with the precipitation anomalies are found west of the dateline (Fig. 3g). However, at this location precipitation itself has little correlation with the leading mode of SST (Fig. 3f). For τ_y, the best correlation is found with the PC of SST in the eastern and northern tropical Pacific (Fig. 3j), and with the PC of precipitation in the western tropical Pacific (Fig. 3i) where once again precipitation itself is not highly correlated with the PC of SST.

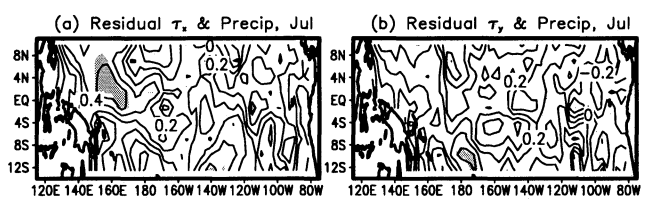

Figure 4. Correlations between the residuals of surface wind stress and precipitation anomalies in July for (a) τ_x and (b) τ_y. Areas with correlations significant at the 1% level for a Student's t-test are shaded.

Table 1. Correlation Coefficients Between the Leading-Mode PCs of the Observed SST, FSU τ_x and τ_y, and *Xie and Arkin* [1997] Precipitation. Values at Better Than the 0.1% Level of Statistical Significance for a Student's t-Test are Shown in Bold.

	(τ_x, SST)	(τ_y, SST)	(τ_x, precip)	(τ_y, precip)	(precip, SST)
Jan	**0.83**	**0.88**	**0.89**	**0.88**	**0.89**
Feb	**0.84**	**0.86**	**0.82**	**0.82**	**0.85**
Mar	0.45	**0.67**	0.59	**0.85**	**0.72**
Apr	0.47	0.62	**0.77**	**0.90**	0.62
May	0.13	0.65	0.25	**0.76**	**0.90**
Jun	0.37	**0.81**	0.56	**0.82**	**0.85**
Jul	0.39	**0.79**	0.63	**0.79**	**0.82**
Aug	0.49	**0.82**	0.61	**0.91**	**0.86**
Sep	0.53	**0.72**	0.63	**0.72**	**0.93**
Oct	**0.83**	**0.82**	**0.85**	**0.83**	**0.97**
Nov	**0.77**	**0.85**	**0.77**	**0.88**	**0.88**
Dec	**0.67**	**0.92**	**0.85**	**0.86**	**0.87**

To elaborate the relations between wind stress and precipitation anomalies during July further, we calculated the correlation between the residuals of τ_x (τ_y) and precipitation anomaly at each grid point (Fig. 4). The residual anomalies for these variables are obtained by subtracting the part that is linearly related to the leading mode of SST variability. The residual τ_x and residual precipitation anomalies correlate significantly in the warm pool region. Comparing Figs. 3g, 3h and 4a one can see that while τ_x anomalies east of the dateline are linked to the leading mode of SST, over the warm pool region τ_x anomalies are primarily determined by precipitation anomalies which are not linearly correlated to the leading modes of SST.

From the above analyses we hypothesize that in January the observed large-scale τ_x and τ_y variability in the central and eastern tropical Pacific is dominated by the large-scale precipitation variability in the central tropical Pacific, which in turn is due to the leading mode of the observed SST variability. In July, the largest SST variability is located at the eastern tropical Pacific. Its significant control over the observed precipitation variability, and hence, τ_x variability are confined in a small area to the central to eastern tropical Pacific. In the western tropical Pacific, the observed precipitation variability, which has no significant relation to the observed SST variability, generates τ_x anomalies west of the dateline.

To check the robustness of our results, instead of using precipitation we repeated the analysis using outgoing long-wave radiation (OLR) from satellite observations from 1979

Table 2. As Table 1, Except for the NCEP/NCAR Reanalysis Wind Stresses and Precipitation.

	(τ_x, SST)	(τ_y, SST)	(τ_x, precip)	(τ_y, precip)	(precip, SST)
Jan	**0.75**	**0.86**	**0.60**	**0.90**	**0.90**
Jul	0.33	**0.72**	**0.63**	0.42	0.41

through 1999. We obtained almost the same correlations shown in Table 1 with precipitation replaced by OLR. We also performed a similar analysis using the surface wind stresses and precipitation of the NCEP/NCAR reanalysis from 1958 through 1999 [*Kalnay et al.*, 1996], and the SST data for the 1958-1999 period. In January, the spatial distributions of leading EOFs of precipitation, τ_x and τ_y from the reanalysis are in good agreement with observed precipitation [*Xie and Arkin*, 1997] and FSU wind stresses (not shown). In July, the centers of the leading EOFs of precipitation and τ_x are respectively located at 160°W and 140°W, about 40° to 60° east to those of the *Xie and Arkin* [1997] precipitation and FSU τ_x (see Figs. 1f and 1g). The leading EOF of τ_y has a similar spatial distribution but smaller magnitude than that of the FSU τ_y. In spite of the differences between the reanalysis and the observational data used in the earlier analysis, we still find that the surface wind stresses are more closely related to SST in January than in July. Shown in Table 2 are the correlation coefficients in January and July between the PCs of the leading EOFs of τ_x, τ_y, precipitation and SST. The correlation coefficient between the PCs of τ_x and SST reaches 0.75 in January and is only 0.33 in July.

4. Conclusion

Seasonality in the dependence of interannual variability of surface wind stress on SST and precipitation over the tropical Pacific is examined using observed data. The analysis was motivated by the fact that for a coupled prediction of ENSO, surface wind stress variability plays a dominant role, and has to be correctly modeled. The major finding of this study is that there is a strong seasonality in the relationships between the leading modes of variability of surface wind stresses and SST or precipitation field. In January, the largest SST anomalies are located in the central and eastern tropical Pacific and the largest precipitation anomalies are located in the central tropical Pacific. The leading modes of τ_x and τ_y anomalies are both significantly correlated with the leading modes of precipitation and SST. In contrast during July, while the largest SST anomalies are located near the coast of South America, the largest precipitation anomalies are located in the western tropical Pacific. In the central to eastern tropical Pacific, τ_x anomalies have little dependence on the SST anomalies. In the western tropical Pacific, τ_x anomalies depend strongly on local precipitation anomalies, although the precipitation variability itself is no longer linked to the leading modes of SST. In other words, during the summer months, surface wind stress variability is less constrained by instantaneous SST variability.

The relationship among the anomalous surface wind stresses, SST and precipitation and its seasonal characteristics found in this study have some implications for ENSO forecast models in which surface wind stress anomalies are diagnosed based on their statistical relations with SST anomalies. This analysis shows that in January both τ_x and τ_y anomalies can be parameterized as a function of SST anomalies in the tropical Pacific. However, during July the specification of τ_x may be more problematic.

Acknowledgments. The support offered by NOAA's Climate Dynamics and Experimental Prediction (CDEP) Program is gratefully acknowledged. We would also like to thank G. H. White, H. M. van den Dool and the two anonymous reviewers for their constructive and thoughtful comments.

References

Barnett, T. P., M. Latif, N. Graham, M. Flugel, S. Pazan, and W. White, ENSO and ENSO-related predictability: Part I - Prediction of equatorial Pacific sea surface temperature with a hybrid coupled ocean-atmosphere model, *J. Clim., 6*, 1545-1566, 1993.

Kalnay, E., and Co-authors, The NCEP/NCAR 40-year reanalysis project, *Bull. Amer. Meteor. Soc., 77*, 437-471, 1996.

Gill, A. E., Some simple solutions for heat induced tropical circulation, *Q. J. Roy. Meteorol. Soc., 106*, 447-462, 1980.

Goldenberg, S. B., and J. J. O'Brien, Time and space variability of the tropical Pacific wind stress, *Mon. Wea. Rev., 109*, 1190-1207, 1981.

Ji, M., A. Kumar, and A. Leetmaa, An experimental coupled forecast system at the National Meteorological Center: Some early results, *Tellus, 46A*, 398-418, 1994.

Kirtman, B. P., J. Shukla, B. Huang, Z. Zhu, and E. K. Schneider, Mutiseasonal predictions with a coupled tropical ocean global atmosphere systems, *Mon. Wea. Rev., 125*, 789-808, 1996.

Lindzen, R. S., and S. Nigam, On the role of sea surface temperature gradients in forcing low level winds and convergence in the tropics, *J. Atmos. Sci., 44*, 2418-2436, 1987.

Reynolds, R. W., and T. M. Smith, Improved global sea surface temperature analyses using optimum interpolation, *J. Clim., 7*, 929-948, 1994.

Smith, T. M., R. W. Reynolds, R. E. Livezey, and D. C. Stokes, Reconstruction of historical sea surface temperature using empirical orthogonal functions, *J. Clim., 9*, 1403-1420, 1996.

Stockdale, T. N., A. J. Busalacchi, D. E. Harrison, and R. Seager, Ocean modeling for ENSO, *J. Geophys. Res., 103*, 14,325-14,355, 1998.

Trenberth, K. E., G. W. Branstator, D. Karoly, A. Kumar, N.-C. Lau, and C. Ropelewski, Progress during TOGA in understanding and modeling global teleconnections associated with tropical sea surface temperature, *J. Geophys. Res., 103*, 14,291-14,324, 1998.

Xie, P., and P. Arkin, Global precipitation: A 17-year monthly analysis based on gauge observations, satellite estimates, and numerical model outputs, *Bull. Amer. Meteor. Soc., 78*, 2539-2558, 1997.

Zebiak, S. E., and M. A. Cane, A model El Niño-Southern Oscillation, *Mon. Wea. Rev., 115*, 2262-2278, 1987.

F. Yang, A. Kumar, and W. Wang, Environmental Modeling Center, National Centers for Environmental Prediction, 5200 Auth Road, Camp Springs, MD 20746, USA. (fyang@ncep.noaa.gov; akumar@ncep.noaa.gov; wwang@ncep.noaa.gov.)

(Received March 8, 2001; revised May 3, 2001;
accepted May 18, 2001.)